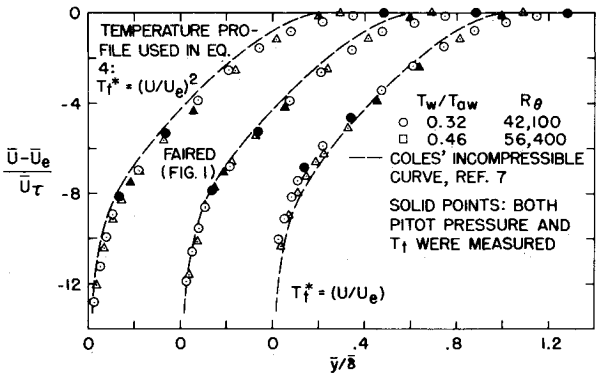

Fig. 3 Effect of changing the temperature-velocity distribution used in Eq. (4) on the velocity-defect law; $M_e = 7.4$.

obtained by fairing the measured temperatures to the finite-difference curve (dashed curve in Fig. 1). This faired curve, the Crocco and the quadratic representations were used in the figures that follow.

Velocity Profile Generalization

Figures 2 and 3 present the results from using Eqs. (4–6) with two velocity profiles from Ref. 6. Figure 2 shows that the assumed Crocco or quadratic temperature profiles do not transform the measured velocity profiles onto the Coles' incompressible curve. On the other hand, the faired experimental temperature distribution transforms the velocity profiles close to Coles' curve. In Fig. 3, the velocity-defect transformations lie close to the Coles' incompressible curve for all temperature distributions. The good correlation with Coles' curve in Fig. 2 obtained by using the modified Van Driest equations indicates that these equations can be applied to obtain skin friction from non-Crocco velocity profiles (Clauser technique) when $T(U)$ is known.

Skin-Friction Generalization

Figure 4 shows a comparison of the predicted and experimental skin friction using Eqs. (7) and (8). Measured R_θ was used in Eq. (8). Theoretical skin-friction values are greatly affected by the different temperature-velocity distributions, as shown by the large differences in the predicted skin friction. Using the faired experimental temperature-velocity curves, the skin friction is predicted to within about 3% of the measured values.

Thus, on the basis of these limited measurements, it appears that the Van Driest method can be extended to the prediction of non-Crocco type turbulent boundary-layer velocity profiles and skin friction by using a modified temperature-velocity distribution in the Van Driest equations.

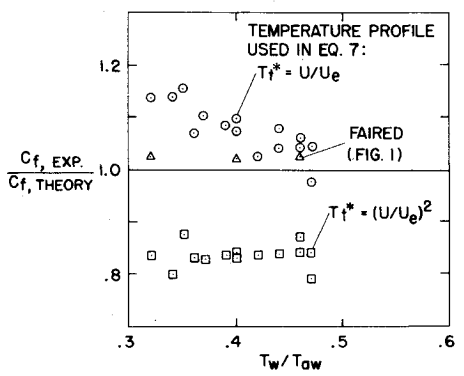

Fig. 4 Effect of changing the temperature-velocity distribution used in Eq. (7) on the prediction of skin friction; $M_e = 7.4$.

References

[1] Van Driest, E. R., "Turbulent Boundary Layer in Compressible Fluids," *Journal of Aeronautical Science*, Vol. 18, No. 3, March 1951, pp. 145–160.

[2] Van Driest, E. R., "The Problem of Aerodynamic Heating," Aerodynamic Aspects Session, National Summer Meeting, IAS, Los Angeles, June 1956.

[3] Hopkins, E. J. and Inouye, M., "An Evaluation of Theories for Predicting Turbulent Skin Friction and Heat Transfer on Flat Plates at Supersonic and Hypersonic Mach Numbers," *AIAA Journal*, Vol. 9, No. 6, June 1971, pp. 993–1003.

[4] Hopkins, E. J., Keener, E. R., Polek, T. E., and Dwyer, H. A., "Turbulent Skin Friction and Boundary-Layer Profiles Measured on Nonadiabatic Flat Plates at Hypersonic Mach Numbers," *AIAA Journal*, Vol. 10, No. 1, Jan. 1972, pp. 40–48.

[5] Keener, E. R. and Hopkins, E. J., "Turbulent Boundary-Layer Velocity Profiles on a Non-Adiabatic Flat Plate at Mach Number 6.5," TN D-6907, 1972, NASA.

[6] Hopkins, E. J. and Keener, E. R., "Pressure-Gradient Effects on Hypersonic Turbulent Skin Friction and Boundary Layer Profiles," *AIAA Journal*, Vol. 10, No. 9, Sept. 1972, pp. 1141–1142.

[7] Coles, D., "Measurements in the Boundary Layer on a Smooth Flat Plate in Supersonic Flow. I. The Problem of the Turbulent Boundary Layer," Rept. 20–69, 1953, Jet Propulsion Lab., California Inst. of Technology, Pasadena, Calif.

[8] Bushnell, D. M., Johnson, C. B., Harvey, W. D., and Feller, E. V., "Comparison of Prediction Methods and Studies of Relaxation in Hypersonic Turbulent Boundary Layers," TN D-5433, 1969, NASA.

Hypersonic Flight Results Showing Reynolds-Number Influence on Turbulent Base Pressure

BRUCE M. BULMER*
Sandia Laboratories, Albuquerque, N.Mex.

Nomenclature

A	= base area
D_s/D_b	= ratio of sting-to-model-base diameter
$\dot{m}$	= total heatshield ablation (mass-addition) rate
$\dot{m}/\rho_\infty V_\infty A$	= mass-addition parameter
M	= Mach number
p	= static pressure
R	= base radial coordinate
R_b, R_n	= base, nose radius
R_n/R_b	= bluntness ratio
Re	= Reynolds number
V	= velocity
θ_c	= cone half-angle
ρ	= static density

Subscripts

b	= base condition
e	= local cone (boundary-layer edge) condition immediately preceding base at L
L	= based on wetted length of cone
∞	= freestream condition

Introduction

THE base pressure of slender ($\theta_c < 15°$) conical re-entry bodies in turbulent flow at zero angle of attack may depend upon several variables: body geometry (θ_c, R_n/R_b, and

Received July 11, 1973. This work was jointly supported by the U.S. Atomic Energy Commission and the U.S. Air Force.

Index categories: Entry Vehicle Testing; Boundary Layers and Convective Heat Transfer—Turbulent; Jets, Wakes, and Viscid-Inviscid Flow Interactions.

*Member, Technical Staff, Re-Entry Vehicle Aerothermodynamics Division. Member AIAA.

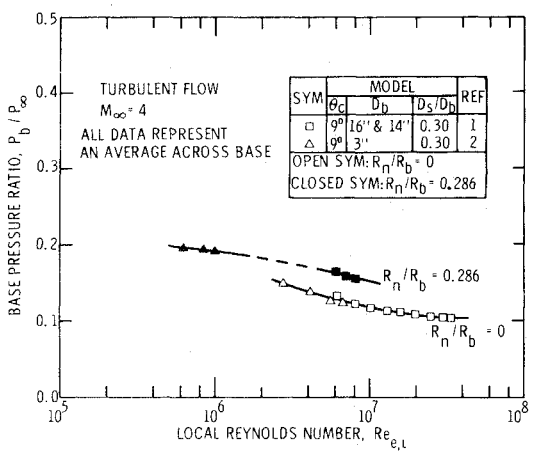

Fig. 1 Ground-test base pressure measurements for sharp and blunt 9° cones at $M_\infty = 4$.

base configuration), freestream Mach number M_∞, freestream Reynolds number $Re_{\infty,L}$, and, if heatshield ablation occurs, mass addition $\dot{m}/\rho_\infty V_\infty A$. For sphere-cone configurations, the turbulent base pressure ratio p_b/p_∞ is a strong function of both body geometry and freestream Mach number; in the hypersonic flow regime, p_b/p_∞ increases with increasing θ_c and R_n/R_b at constant Mach number and with increasing M_∞ for a given body geometry.[1-4] The effect of heatshield ablation on the turbulent base pressure of full-scale re-entry vehicles (RV's) is to increase p_b/p_∞ above the zero-mass-addition level and to create radial p_b/p_∞ gradients.[4-6] With regard to freestream Reynolds number, p_b/p_∞ tends toward a constant level for sufficiently large $Re_{\infty,L}$ (thin boundary layers).[1,2,7] Therefore, it is generally assumed that p_b/p_∞ is specified for a given body geometry, M_∞, and $\dot{m}/\rho_\infty V_\infty A$, with $Re_{\infty,L}$ being eliminated per se when large values of that parameter are considered.

Whitfield and Potter[1] demonstrated in 1960, for sharp and spherically blunted cones at $M_\infty = 2$–5, that p_b/p_∞ becomes nearly constant for high local Reynolds number (i.e., $Re_{e,L}$ in excess of 4×10^7, approximately). For sharp bodies, high $Re_{e,L}$ can generally be achieved because $Re_{e,L}$ may be (depending upon θ_c and M_∞) several times the corresponding freestream value. However, for blunt cones in turbulent flow ($R_n/R_b > 0.1$), $Re_{e,L}$ can be a small fraction (possibly 10% or less) of $Re_{\infty,L}$ as a result of entropy-layer effects arising from the curved bow shock. Therefore, the condition $Re_{e,L} \geqq 4 \times 10^7$ may require $Re_{\infty,L}$ to be as large as 4×10^8 or more for blunt cones.

If the approximate condition $Re_{e,L} \geqq 4 \times 10^7$ is not achieved, whether on sharp or blunt cones, turbulent p_b/p_∞ may display a considerable dependence upon $Re_{e,L}$. This Reynolds-number influence is illustrated in Fig. 1 for several 9° half-angle sharp and blunt sting-supported models at $M_\infty = 4$. For two different geometrical shapes, the data of Whitfield and Potter and of Zarin[2] show agreement (all data are for the same sting-to-base-diameter ratio D_s/D_b) and exhibit a substantial variation with Reynolds number. For the sharp cones, the base pressure ratio becomes constant for large $Re_{e,L}$, but a 40% variation in p_b/p_∞ from the asymptotic high-Reynolds-number value is observed as $Re_{e,L}$ is decreased. The Reynolds-number effect is even more pronounced for the blunt cones, with the reduced values of $Re_{e,L}$ being below those required to obtain constant p_b/p_∞.

Figure 1 illustrates the Reynolds-number influence observed in ground-test data at lower M_∞. The significance of this effect becomes apparent in the extrapolation of ground-test data to flight conditions and in the application of flight-test data to other flight conditions[8]; therefore, it is of practical interest to investigate the effect of Reynolds number on the turbulent base pressure of slender conical bodies during atmospheric re-entry. To this end, flight-test base pressure data from three slightly blunt ($R_n/R_b = 0.05$) slender RV's and from one very blunt ($R_n/R_b = 0.3$) slender RV are presented to illustrate the Reynolds-number influence on full-scale vehicles at hypersonic ($M_\infty \approx 15$ and 10.5) Mach numbers. It is shown that the 5% blunt RV's are sufficiently sharp in turbulent flow that Reynolds number has no effect on p_b/p_∞, whereas the 30% blunt vehicle is sufficiently blunt that an appreciable Reynolds-number dependence is seen in turbulent flow.

Re-entry Vehicles, Instrumentation, and Data Reduction

The 5% blunt vehicles were similar 9° cones with essentially flat bases and ablative heatshields. Flow conditions were turbulent at $M_\infty \approx 15$ for all three RV's. Base pressures were measured slightly off-centerline ($R/R_b = 0.1$) with a 0–1 psia range variable-reluctance transducer (Flight 1) and with 0–50 torr range thermal-conductivity transducers (Flights 2 and 3). The 30% blunt RV had a flat base and a nonablative heatshield. The flow was turbulent at $M_\infty = 10.5$, and a potentiometric transducer recorded the base pressure at $R/R_b = 0.45$.

The angle of attack was nominally zero for all flights. Atmospheric conditions derived from radiosonde data were utilized in calculated trajectories that included telemetered acceleration data to determine the necessary freestream parameters ($M_\infty, Re_{\infty,L}$, etc.) for each flight. Calculations of the boundary-layer edge (local) conditions on the cone frustum immediately preceding the base included real-gas effects and entropy-layer and pressure-overexpansion (bluntness) effects.[9]

Results

Data from the 5% blunt RV's are shown in Fig. 2 in terms of both $Re_{\infty,L}$ and $Re_{e,L}$. Turbulent flow was verified by heatshield temperature and base calorimeter data telemetered during each flight. Note that the body geometry (θ_c and R_n/R_b) and measurement location (R/R_b) were the same for all three vehicles, and, in particular, note that the freestream Mach number and mass-addition parameter are constant for each set of data and are identical for the three flights ($M_\infty \approx 15$, $\dot{m}/\rho_\infty V_\infty A \approx 0.0012$). Therefore, these data are directly comparable in terms of Reynolds number only.

The data in Fig. 2 reveal no variation in p_b/p_∞ with Reynolds number for $6.3 \times 10^7 \leqq Re_{\infty,L} \leqq 1.6 \times 10^8$. The corresponding $Re_{e,L}$ varies from 1.7×10^8 to 3.5×10^8 (approximately 2 to 2.5 times $Re_{\infty,L}$) and is far in excess of 4×10^7; accordingly, based upon the conclusions of Whitfield and Potter, no Reynolds-number dependence is expected for these data. These results at $M_\infty \approx 15$ are similar to $M_\infty \approx 21$ RV flight data[10] from a sharp 10° ablating cone, for which no variation in p_b/p_∞ was seen for $Re_{\infty,L} = 1.0$–2.4×10^8.

Base pressure data from the 30% blunt, slender, nonablating ($\dot{m} = 0$) RV at $M_\infty = 10.5$ are presented in Fig. 3 in terms of the base-to-local-cone-pressure ratio p_b/p_e and $Re_{e,L}$. Turbulent flow

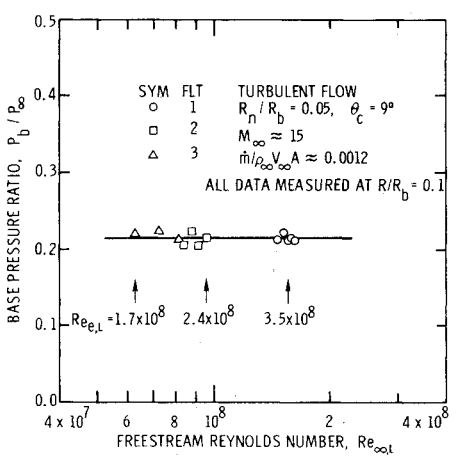

Fig. 2 Flight-test base pressure data, $R_n/R_b = 0.05$.

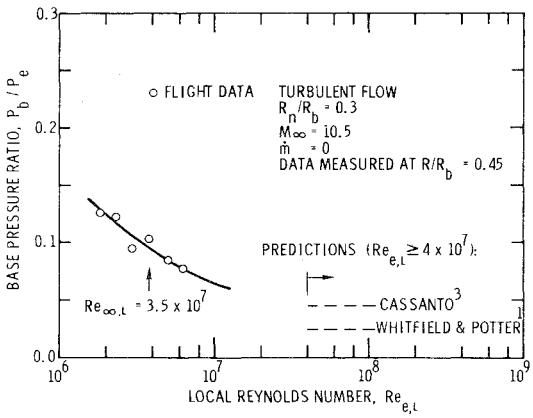

Fig. 3 Flight-test base pressure data, $R_n/R_b = 0.3$.

on the RV was verified by telemetered heatshield calorimeter data. Note that $Re_{e,L}$ varies from 1.9×10^6 to 6.3×10^6 and is, owing to the bluntness of this vehicle, only about 10% of the corresponding $Re_{\infty,L}$. Because the $Re_{e,L}$ is considerabiy less than 4×10^7, a significant Reynolds-number effect is expected on the basis of the Whitfield and Potter conclusions.

High-Reynolds-number predictions[1,3] for the $M_\infty = 10.5$ data are also included in Fig. 3. Reasons for the discrepancy between these two semiempirical predictions have been discussed by Cassanto and Mendelson;[11] hence, it suffices only to point out that both methods indicate a base pressure level considerably lower than what was in fact measured. The rather severe variation ($\sim 60\%$) in p_b/p_e seen for $Re_{e,L} \leqq 6.3 \times 10^6$ illustrates the Reynolds-number influence on a full-scale hypersonic flight vehicle.

Conclusions

The influence of Reynolds number on turbulent base pressure has been discussed relative to hypersonic re-entry. Flight data from slightly blunt slender cones, for which $Re_{e,L} \gg 4 \times 10^7$ ($Re_{e,L} \approx 2Re_{\infty,L}$), reveal no Reynolds-number effect, whereas an appreciable Reynolds-number dependence ($\sim 60\%$ variation) is shown for a very blunt slender cone for which $Re_{e,L} \ll 4 \times 10^7$ ($Re_{e,L} \approx 0.1\, Re_{\infty,L}$). These hypersonic ($M_\infty \approx 15$ and 10.5) results are consistent with the ground-test data of Whitfield and Potter for $M_\infty = 2$–5 and support the conclusion that, unless $Re_{e,L}$ is sufficiently large, Reynolds-number variations may strongly influence the turbulent base pressure of full-scale vehicles during re-entry.

References

[1] Whitfield, J. D. and Potter, J. L., "On Base Pressures at High Reynolds Numbers and Hypersonic Mach Numbers," AEDC-TN-60-61, March 1960, Arnold Engineering Development Center, Tullahoma, Tenn.

[2] Zarin, N. A., "Base Pressure Measurements on Sharp and Blunt 9° Cones at Mach Numbers from 3.50 to 9.20," *AIAA Journal*, Vol. 4, No. 4, April 1966, pp. 743–745.

[3] Cassanto, J. M., "Effect of Cone Angle and Bluntness Ratio on Base Pressure," *AIAA Journal*, Vol. 3, No. 12, Dec. 1965, pp. 2351–2352.

[4] Cassanto, J. M. and Storer, E. M., "A Revised Technique for Predicting the Base Pressure of Sphere Cone Configurations in Turbulent Flow Including Mass Addition Effects," ALFM 68-41, Oct. 1968, Re-Entry Systems Dept., General Electric Co., Philadelphia, Pa.

[5] Cassanto, J. M. and Hoyt, T. L., "Flight Results Showing the Effect of Mass Addition on Base Pressure," *AIAA Journal*, Vol. 8, No. 9, Sept. 1970, pp. 1705–1707.

[6] Bulmer, B. M., "Effect of Low Heat-Shield Ablation Rates on Flight Test Turbulent Base Pressure," *AIAA Journal*, Vol. 10, No. 12, Dec. 1972, pp. 1704–1705.

[7] Cassanto, J. M., "Base Pressure Results at $M = 4$ Using Free-Flight and Sting-Supported Models," *AIAA Journal*, Vol. 6, No. 7, July 1968, pp. 1411–1414.

[8] Hayos, F. G., "Turbulent Boundary-Layer Effects on Base Pressure," *Journal of the Aeronautical Sciences*, Vol. 24, No. 10, Oct. 1957, pp. 781–782.

[9] Hochrein, G. J., "A Procedure for Computing Aerodynamic Heating on Sphere Cones—Program BLUNTY," SC-DR-69-449, Nov. 1969, Sandia Labs., Albuquerque, N. Mex.

[10] Cassanto, J. M., "Flight Test Base Pressure Results at Hypersonic Mach Numbers in Turbulent Flow," *AIAA Journal*, Vol. 10, No. 3, March 1972, pp. 329–331.

[11] Cassanto, J. M. and Mendelson, R. S., "Local Flow Effects on Base Pressure," *AIAA Journal*, Vol. 6, No. 6, June 1968, pp. 1182–1185.

Spherically-Symmetric Supersonic Source Flow: A New Use For The Prandtl-Meyer Function

WALTER F. REDDALL III*
The Aerospace Corporation, El Segundo, Calif.

Introduction

INVISCID supersonic flow with spherical symmetry is so simple that it seems to deserve more attention than it has been given in most textbooks on gas dynamics. This is particularly true in light of the fact that investigators who study the plume generated by a rocket exhaust frequently appeal to supersonic source flow as the limit reached by the flow far downstream of the nozzle, and also as a simplification of the flow in the nozzle itself near the exit plane.

The conditions in a conical, divergent nozzle of half-angle θ_N need not be uniform in the conical coordinate θ, but when the assumption is made that they are, the dependent variables become functions only of the radial coordinate R, measured from the virtual origin of the cone. In this case the flow bounded by the nozzle wall fits the requirements of quasi-one-dimensional isentropic motion. The streamlines in such a flow are radial lines, and the flow can only exist in the domain $R > R^*$, where R^* is the radius at which sonic conditions exist (c.f. Courant and Friedrichs, pp. 377–380). The characteristics, however, are curves in (R, θ) space (see Fig. 1), the equations for which are not well documented, if at all. This Note presents a derivation of those equations for the case of a perfect gas, using the local Mach number as a curve parameter. A generalization to any real gas is also provided. The results reveal that the change in streamline slope θ between any two points on a characteristic is equal to half the change in the Prandtl-Meyer function between the same two points. This is in contrast to the case of radial supersonic flow in a plane, where the change in θ along a physical characteristic is equal to the change in Prandtl-Meyer function. (The image of such a radial-flow characteristic in the hodograph plane is an epicycloid of the same family.) The connection thus established between a function thought to have application only to plane flows and a spherically-symmetric flow is the most interesting feature of the analysis.

The exact relations for the characteristics may be valuable, as are most exact solutions, as a standard for measuring the error of approximate solutions. For example, a method-of-characteristics computer code could be given the simple task of computing a conical flow starting from a set of exact conditions at some initial station R_i, and the departure of the computed

Received July 12, 1973; revision received August 13, 1973.
Index category: Supersonic and Hypersonic Flow.
* Member of Technical Staff.